



Study of non-covalent interaction between a designed monoporphyrin and fullerenes (C_{60} and C_{70}) in absence and presence of silver nanoparticles

Ratul Mitra^a, Ajoy K. Bauri^b, Sumanta Bhattacharya^{a,*}

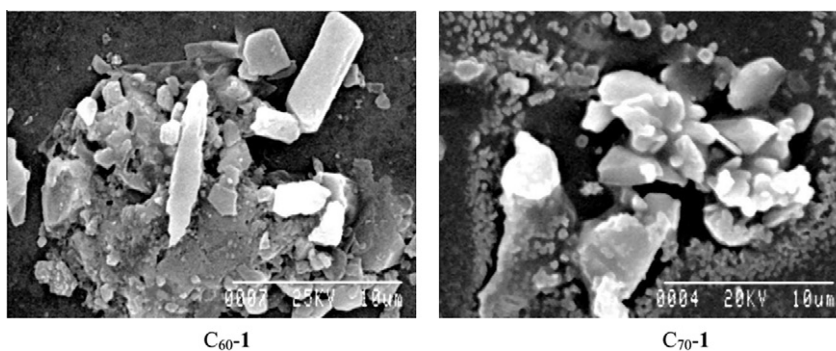
^a Department of Chemistry, The University of Burdwan, Golapbag, Burdwan 713 104, India

^b Bio-Organic Division, Bhabha Atomic Research Centre, Trombay, Mumbai 400 085, India

HIGHLIGHTS

- ▶ Fullerene-porphyrin complexation is examined in presence of silver nanoparticles.
- ▶ Silver nanoparticles (AgNp) inhibit binding between fullerene and porphyrin (**1**).
- ▶ DLS study reveals larger size particles of AgNp in presence of fullerene-**1** complex.
- ▶ SEM measurements establish formation of surface holes in fullerene-**1**-AgNp structure.
- ▶ Electrostatic attraction between porphyrin-based supramolecule and AgNp is observed.

GRAPHICAL ABSTRACT



ARTICLE INFO

Article history:

Received 17 February 2012

Received in revised form 6 May 2012

Accepted 17 May 2012

Available online 24 May 2012

Keywords:

Fullerenes

Monoporphyrin **1**

Silver nanoparticle

UV-Vis and steady state fluorescence studies

SEM

DLS

ABSTRACT

The present article reports on supramolecular interaction between fullerenes (C_{60} and C_{70}) and a designed monoporphyrin, e.g., 5,15-di(para-methoxyphenyl)zincporphyrin (**1**), in absence and presence of silver nanoparticles (AgNp) having diameter of ~ 3 – 7 nm in toluene. While UV-Vis studies establish the ground state electronic interaction between fullerenes and **1** in absence and presence of AgNp, steady state fluorescence experiment enables us to determine the value of binding constant (K) for the fullerene-**1** complexes in solution. Steady state fluorescence measurement reveals that reduction in the K value takes place for both C_{60} -**1** ($K = 1560 \text{ dm}^3 \text{ mol}^{-1}$) and C_{70} -**1** systems ($K = 14,970 \text{ dm}^3 \text{ mol}^{-1}$) in presence of AgNp, i.e., $K_{C_{60}-1} = 1445 \text{ dm}^3 \text{ mol}^{-1}$ and $K_{C_{70}-1} = 14,550 \text{ dm}^3 \text{ mol}^{-1}$. SEM measurements establish formation of surface holes in fullerene-**1**-AgNp structure. Both SEM and dynamic light scattering measurement demonstrates that the electrostatic attraction between porphyrin-based supramolecules and AgNp is very much responsible behind the formation of larger aggregates. Quantum chemical calculations evoke the single projection geometric structures of the fullerene-**1** complexes in vacuo and well interpret the alignment of the C_{60} and C_{70} molecule with the flat -belt region of **1**.

© 2012 Elsevier B.V. All rights reserved.

Introduction

One of the most attractive strategies in recent days is to develop inexpensive and renewable energy resources in terms of the generation of organic solar cells that mimic natural photosynthesis in

the conversion and storage of solar energy [1–3]. Synthetic chemists have made their artificial analogues of photosynthetic reaction centre, namely, porphyrin, which absorb light effectively and can participate in photoinduced charge and energy transfer reactions [4]. In this connection, porphyrin and fullerene have been found to be an ideal donor-acceptor couple, because the combination of these two species results in a small reorganization energy, which allows to accelerate photoinduced electron transfer and to

* Corresponding author. Tel.: +91 335 6327254; fax: +91 342 2530452.

E-mail address: sum_9974@rediffmail.com (S. Bhattacharya).

slow down charge recombination, leading to the generation of a long lived charge-separated state with a high quantum yield [5–10]. Taking into account the fact that fullerene and porphyrin tend to make a supramolecular complex in solutions as well as in the solid state [11–14], and as this type of model system is of great importance not only in opto-electronic technologies [15], but also in life science in relation to respiration [16], photosynthesis [17] and photomedicine [18], it would be a great idea to see whether any photophysical changes take place in the composite mixture containing fullerene and porphyrin when silver nanoparticles (AgNp) are added in such assembly. For the aforesaid reasons, we have designed a monoporphyrin molecule, namely 5,15-di(para-methoxyphenyl)porphyrin metal Zn (**1**) (see Scheme 1 and Scheme 2) to find out its intermolecular interaction with fullerenes C₆₀ and C₇₀ in absence and presence of AgNp. Metal nanoparticles have size dependent optical and electrical properties [19]. In this respect, an important feature of metal nanoparticles is the localized surface plasmon band resonance [20], which is seen as high extinction coefficients of metal nanoparticles. As a result of this, smaller sizes of metal nanoparticles absorb light intensively, whereas scattering of light becomes an important factor for bigger nanoparticles. The surface plasmon band resonance causes enhancement of electromagnetic field near the metal nanoparticles. Applications utilizing the surface plasmon resonances of metal nanoparticles include imaging, sensing, medicine, photonics and optics [21,22]. Although there are some reports on interaction between fullerene and gold nanoparticles (AuNp) in presence of porphyrin in recent past [23,24], there is no such investigation on non-covalent interaction between fullerene and porphyrin in presence of silver nanoparticles (AgNp). In recent past, a novel two-step bottom-up approach to construct a 2-dimensional long-range ordered, covalently bonded fullerene-porphyrin binary nanostructure is presented in presence of Ag(110) [25]. However, we anticipate that the combination of photoactive molecules, like fullerene and porphyrin, into formation of non-covalent assembly in presence of AgNp may lead to some new physicochemical aspects. The motivation of the present work, therefore, deals with the non-covalent interaction between fullerenes and monoporphyrin in presence of AgNp. Binding and selectivity in binding between fullerenes and **1** is one of the goals of our present studies, other than to envisage various physicochemical aspects on host-guest chemistry of fullerene and porphyrin in presence of AgNp.

Materials and methods

C₆₀ and C₇₀ are purchased from Sigma-Aldrich, USA and used without further purification. **1** is synthesized in our laboratory and the detailed synthetic procedures are reported in Supporting Information. The synthetic schemes are demonstrated as Appendix A. UV-vis spectroscopic grade toluene (Merck, Germany) is used as solvent to favor the intermolecular interaction between fullerene and **1**, as well as to provide good solubility and photostability of the samples. UV-vis spectral measurements have been performed on a Shimadzu UV-2450 model spectrophotometer using quartz cell with 1 cm optical path length. Steady state emission spectra are recorded with a Hitachi F-4500 model fluorescence spectrophotometer. DLS measurements have been done with Nano S Malvern instrument employing a 4 mW He-Ne laser ($\lambda = 413$ nm) equipped with a thermostated sample chamber. All the scattered photons are collected at 173° scattering angle. SEM measurements are done in a S-530 model of Hitachi, Japan instrument having IB-2 ion coater with gold coating facility.

Results and discussions

UV-Vis investigations

The ground state absorption spectrum of **1** (1.880×10^{-6} mol dm⁻³, Fig. 1(i)) in toluene recorded against the solvent as reference displays one broad Soret absorption band ($\lambda_{\text{max}} = 413$ nm) corresponding to the transition to the second excited singlet state S₂. As for the Q absorption bands, **1** shows one major absorption band at 540 nm and one minor band at 503 nm (Fig. 1(i)). Q absorption bands in metalloporphyrin correspond to the vibronic sequence of the transition to the lowest excited singlet state S₁. The inset of Fig. 1, i.e., Fig. 1(ii), shows the electronic absorption spectrum of 0.02 ml AgNp solution in 4 ml toluene measured against toluene. The distinctive color of AgNp is due to a phenomenon known as plasmon absorbance. Incident light creates oscillations in conduction electrons on the surface of the nanoparticles and electromagnetic radiation is absorbed. The spectrum of the clear yellow colloidal silver shows distinct absorption band near the region of 443 nm due to its surface plasmon band resonance character [26]. When 0.02 ml solution of AgNp is added to the solution of **1** (1.880×10^{-6} mol dm⁻³) and the electronic absorption spectrum of the mixture is recorded against the same concentration of AgNp in toluene, the intensity of the Soret absorption band is found to decrease from absorbance value of 0.765–0.678 (Fig. 1(iii)). In our present work, we have made a detailed study how the surface plasmon band resonance of AgNp is affected in presence of only fullerene, only porphyrin and fullerene-porphyrin mixture. Fig. 1S shows the UV-Vis absorption spectrum of AgNp in toluene measured against the solvent as reference which is shown in blue color ink. The red spectrum shows the electronic spectrum of blank C₆₀ in toluene recorded against the solvent as reference. The sky blue spectrum corresponds to the spectrum of mixture of C₆₀ and AgNp recorded against the solvent as reference. It is observed that AgNp gets 7 nm red shift in its peak maxima following the addition of C₆₀. However, in presence of only **1** (magenta color spectrum) and C₆₀-**1** binary mixture (black colour spectrum), there is no change observed either in peak maxima or in intensity of the peak. In both the cases mentioned above, we have not detected the presence of any sort of additional absorption peak, which also indicates absence of charge transfer (CT) phenomenon in our present studies. However, we may observe somewhat shouldering in the absorption spectrum of C₆₀-**1**-AgNp composite around 465 nm. Almost, similar sort of absorption spectral feature for the surface plasmon band resonance of AgNp is observed in presence of C₇₀ and C₇₀-**1** mixture recorded in toluene (Fig. 2S). However, in presence of only C₇₀, the surface plasmon band resonance of AgNp gets 21 nm red shift which is 14 nm larger compared to C₆₀. The most interesting feature of the UV-Vis experiment of the C₇₀-**1**-AgNp mixture is that the shouldering in the UV-Vis spectrum that we observe in case of C₆₀-**1** composite, appears as a distinct peak; the peak maximum is observed at 467 nm. Evidence in favor of ground state electronic interaction between fullerenes and **1** first comes from the UV-Vis titration experiment. It is observed that addition of a C₆₀ (1.0×10^{-5} mol dm⁻³) and C₇₀ solution (1.0×10^{-5} mol dm⁻³) to a toluene solution of **1** (1.10×10^{-5} mol dm⁻³) decreases the absorbance value of **1** at its Soret absorption maximum (inset of Fig. 3S and Fig. 2, respectively) recorded against the pristine acceptor solution as reference; the extent of decrease is considerably larger in magnitude compared to AgNp in toluene. However, no additional absorption peaks are observed in the visible region. The former observation extends a good support in favor of the non-covalent complexation between fullerenes and **1** in ground state. The latter observation indicates that the interaction is not controlled by charge transfer (CT) transition. Another important feature of the UV-Vis investigations is the larger extent of decrease in the absorbance value of **1** in presence of C₇₀ in comparison to C₆₀. This spectroscopic observation suggests greater amount of interaction between C₇₀ and **1**. However, measurements of UV-Vis spectrum of the

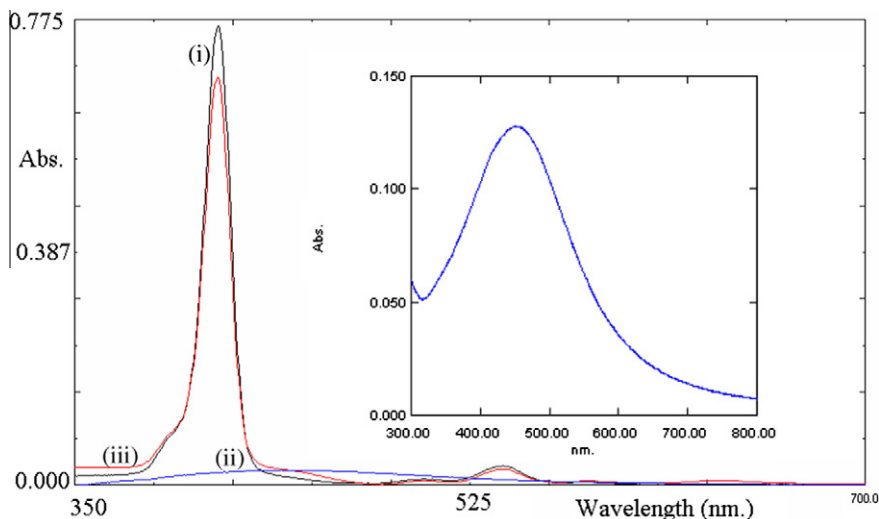


Fig. 1. UV-Vis absorption spectrum of (i) **1** ($1.880 \times 10^{-6} \text{ mol dm}^{-3}$), (ii) AgNp and (iii) **1** ($1.880 \times 10^{-6} \text{ mol dm}^{-3}$) + AgNp mixture in toluene recorded against the solvent containing AgNp as reference.

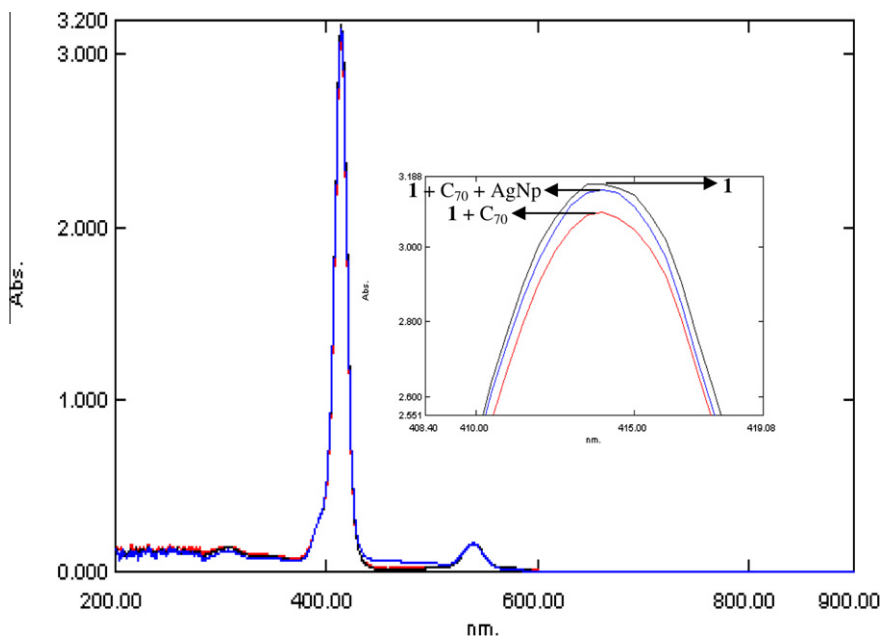


Fig. 2. UV-Vis absorption spectrum of uncomplexed **1** ($1.10 \times 10^{-5} \text{ mol dm}^{-3}$) in toluene recorded against the solvent as reference along with UV-Vis absorption spectrum of C_{70} -**1** system in absence and presence of AgNp maintaining the same condition; inset of Fig. 2 demonstrates the variation in absorbance value of **1** ($1.10 \times 10^{-5} \text{ mol dm}^{-3}$) in presence of C_{70} ($1.0 \times 10^{-5} \text{ mol dm}^{-3}$) + AgNp mixture and C_{70} ($1.0 \times 10^{-5} \text{ mol dm}^{-3}$) solution in toluene only.

C_{60} ($1.0 \times 10^{-5} \text{ mol dm}^{-3}$) + **1** ($1.10 \times 10^{-5} \text{ mol dm}^{-3}$) and C_{70} ($1.0 \times 10^{-5} \text{ mol dm}^{-3}$) + **1** ($1.10 \times 10^{-5} \text{ mol dm}^{-3}$) mixtures in presence of AgNp recorded against the same concentration of fullerene in presence of AgNp, make new physical insight. It is observed that in presence of AgNp, the intensity of the Soret absorption peak of the C_{60} + **1** and C_{70} + **1** mixtures increase (inset of Fig. 3S and Fig. 2, respectively), in comparison to the situation when complexation takes place between **1** and fullerenes in absence of AgNp. From the above observations we may infer that binding phenomenon between C_{60} and **1** takes place at less extent in presence of AgNp. Similar observation is observed in case of C_{70} -**1** complexation process. This new photophysical feature of the fullerene-**1** mixtures in presence of AgNp prompt us to measure the quantitative estimation of the binding phenomenon

between fullerenes and **1** in absence and presence of AgNp employing steady state fluorescence spectroscopic tool.

Steady state fluorescence investigations

The photoinduced behavior of the complexes of the C_{60} -**1** and C_{70} -**1** complexes has been investigated by steady-state emission measurements. It is observed that the fluorescence of **1** upon excitation at Soret absorption band diminishes gradually during titration with C_{60} (Fig. 4S(a)) and C_{70} (Fig. 3) solutions in toluene. This indicates that there is a relaxation pathway from the excited singlet state of the porphyrin to that of the fullerene in toluene. It is already reported that charge separation can also occur from the excited singlet state of the porphyrin to the C_{60} in toluene med-

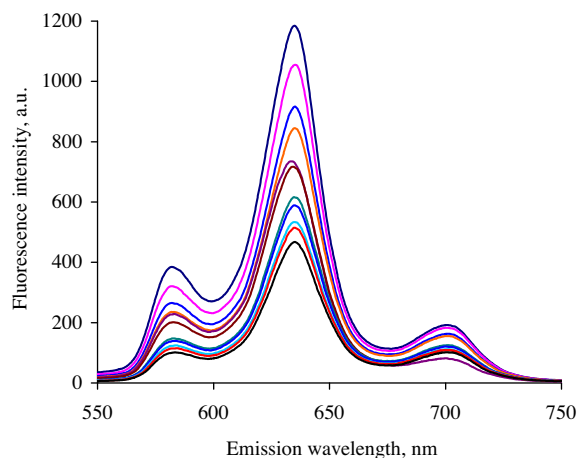


Fig. 3. Steady state fluorescence spectral variation of **1** (3.750×10^{-6} mol dm $^{-3}$) by C $_{60}$ (1.05×10^{-5} – 9.90×10^{-5} mol dm $^{-3}$) in absence of AgNp recorded in toluene.

ium [27]. Competing between the energy and electron transfer processes is a universal phenomenon in donor molecule-fullerene complexes [28], solvent dependent photo physical behavior is a typical phenomenon of the most fullerene-porphyrin dyads studied to date [29]. Photo physical studies already prove that in conformationally flexible fullerene/porphyrin dyad, π -stacking interactions facilitate the through space interactions between these two chromophores which is demonstrated by quenching of 1 porphyrin* fluorescence and formation of fullerene excited states (by energy transfer) or generation of fullerene porphyrin* ion-pair states (by electron transfer) [30]. However, in non-polar solvent, energy transfer generally dominates (over the electron transfer process) the photo physical behavior in deactivating the photo excited chromophore 1 porphyrin* of fullerene-porphyrin dyad. Similar sort of rationale is already proved by Yin et al. for their particular *cis*-2,5-dipyridylpyrrolidino [3,4,1,2] C $_{60}$ -zinc-tetraphenylporphyrin supramolecule [31]. In the present investigation, therefore, the quenching phenomenon can be ascribed to photoinduced energy transfer from porphyrins to fullerenes. As we use the Soret absorption band as our source of excitation wavelength in fluorescence experiment, the 2nd excited singlet state of **1** is deactivated by singlet-singlet energy transfer to the fullerene. Although **1** exhibits fluorescence quenching upon the addition of fullerenes, the quenching efficiency of C $_{70}$ is higher than that of

Table 1

Binding constants (K) for the non-covalent complexes of **1** with C $_{60}$ and C $_{70}$ in absence and presence of AgNp recorded in toluene. Temp. 298 K.

System	K , dm 3 mol $^{-1}$	
	In absence of AgNp	In presence of AgNp
1	–	–
C $_{60}$ - 1	1560 ± 155	1445 ± 145
C $_{70}$ - 1	$14,970 \pm 375$	$14,550 \pm 295$

C $_{60}$. As ground state complex formation between **1** and fullerenes is evidenced from the steady state fluorescence studies, let us consider the formation of a non-fluorescent 1:1 complex according to the equilibrium:



The fluorescence intensity of the solution decreases upon addition of fullerenes C $_{60}$ and C $_{70}$. Using the relation of binding constant (K) we obtain,

$$K = \frac{[\text{Fullerene} - \mathbf{1}]}{[\mathbf{1}][\text{Fullerene}]} \quad (2)$$

Using the mass conservation law, we may write

$$[\mathbf{1}]_0 = [\mathbf{1}] + [\text{Fullerene} - \mathbf{1}] \quad (3)$$

where $[\mathbf{1}]_0$, $[\mathbf{1}]$ and $[\text{Fullerene} - \mathbf{1}]$ are the initial concentrations of **1**, **1** in presence of fullerene, and Fullerene-**1** complex, respectively. Eq. (3) can be rearranged as:

$$\frac{[\mathbf{1}]_0}{[\mathbf{1}]} = 1 + \frac{[\text{Fullerene} - \mathbf{1}]}{[\mathbf{1}]} \quad (4)$$

Using the value of K in place of $[\text{Fullerene} - \mathbf{1}]/[\mathbf{1}]$ from Eq. (2), we can write the Eq. (4) as follows

$$\frac{[\mathbf{1}]_0}{[\mathbf{1}]} = 1 + K[\text{Fullerene}] \quad (5)$$

Considering the fluorescence intensities are proportional to the concentrations, Eq. (5) is expressed as:

$$F_0/F = 1 + K[\text{Fullerene}] \quad (6)$$

where, F_0 is the fluorescence intensity of **1** in the absence of fullerene and F is the fluorescence intensity of **1** in the presence of quencher (i.e., fullerene). In our present investigations, steady-state fluorescence quenching studies afforded excellent linear plot for both the C $_{60}$ -**1** and C $_{70}$ -**1** systems as demonstrated in Fig. 4 (a and b), respectively, which is explained by fluorescence of **1** is being quenched only by static mechanism, as opposed to diffusional

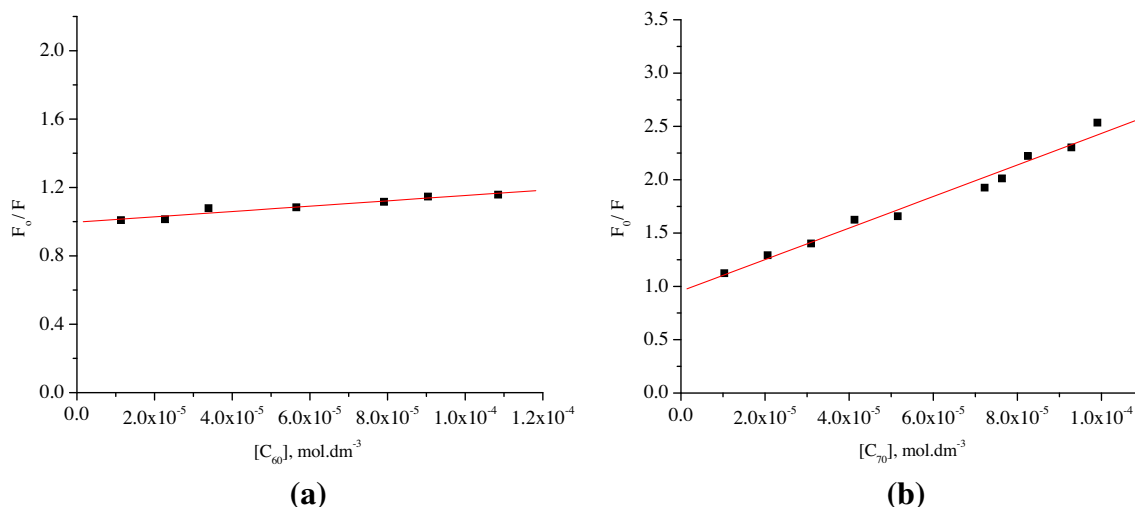


Fig. 4. SV type plots of (a) C $_{60}$ -**1** and (b) C $_{70}$ -**1** systems in absence of AgNp.

quenching process. Eq. (6), therefore, represents a stern–volmer (SV) type plot for investigated supramolecules. K values of the C_{60} –**1** and C_{70} –**1** systems are given in Table 1. The binding constant is determined by the Eq. (6) for the C_{60} –**1** and C_{70} –**1** systems are estimated to be 1560 and 14,970 $\text{dm}^3 \text{mol}^{-1}$, respectively. It is interesting to note that the increase in magnitude of binding constant led to increase of the fluorescence quenching efficiency. Although the details are not clear at this point, the well-defined structure of **1** has afforded tight fixing of C_{60} should give rise to correct host–guest orientation. The steady state fluorescence emission measurements of C_{60} –**1** and C_{70} –**1** systems in presence of AgNp, however, evoke new physicochemical insight regarding perturbation in binding between fullerenes and **1** in solution. It is observed that the K value of C_{60} –**1** and C_{70} –**1** systems in presence of AgNp are estimated to be 1445 and 14550 $\text{dm}^3 \text{mol}^{-1}$, respectively, which are found to be lower in absence of AgNp (see Table 1). This phenomenon clearly suggests that AgNp particles partially cover the surface area of the monoporphyrin which renders the fullerenes C_{60} and C_{70} molecules to un-dergo interaction with **1**. The steady state fluorescence quenching spectral variation of **1** by C_{60} and C_{70} in presence of AgNp are given as Figs. 4S(b) and 5S, respectively; corresponding SV type plots are provided in Figs. 6S(a) and 6S(b), respectively.

Dynamic light scattering experiment

Dynamic light scattering (DLS) is the most versatile and useful set of techniques for measuring in situ on the sizes, size distributions, and (in some cases) the shapes of nanoparticles in liquids [32–34]. In our present investigations, DLS measurements clearly demonstrate that presence of AgNp inhibit the complexation between fullerenes and **1** in toluene. Fig. 7S shows the variation of scattering intensity vs. size of the AgNp solution in presence of **1**. It shows that size of AgNp remains within the range of ~ 5 – 7 nm. Figs. 5 (a and b) show the variation in scattering intensity against the size of the nanoparticles for C_{60} –AgNp and C_{70} –AgNp systems, respectively; from these two figures, it is revealed that the size of the nanoparticles are in the range of ~ 6.5 and ~ 3.75 nm, in presence of C_{60} and C_{70} , respectively. However, in presence of the binary mixtures consisting of C_{60} + **1** (Fig. 5 (c)) and C_{70} + **1** (Fig. 5(d)), the particle size of AgNp is found to be ~ 16.3 nm, in both the cases observed. The above scenario provides strong evidence in favor of the fact that in presence of fullerenes, AgNp partially covers the surface area of porphyrin, which renders the fullerene molecule to undergo interaction with the whole surface area of **1**. This is the reason behind the fact that the magnitude of K of the C_{60} –**1** and C_{70} –**1** systems decreases in presence of AgNp in toluene.

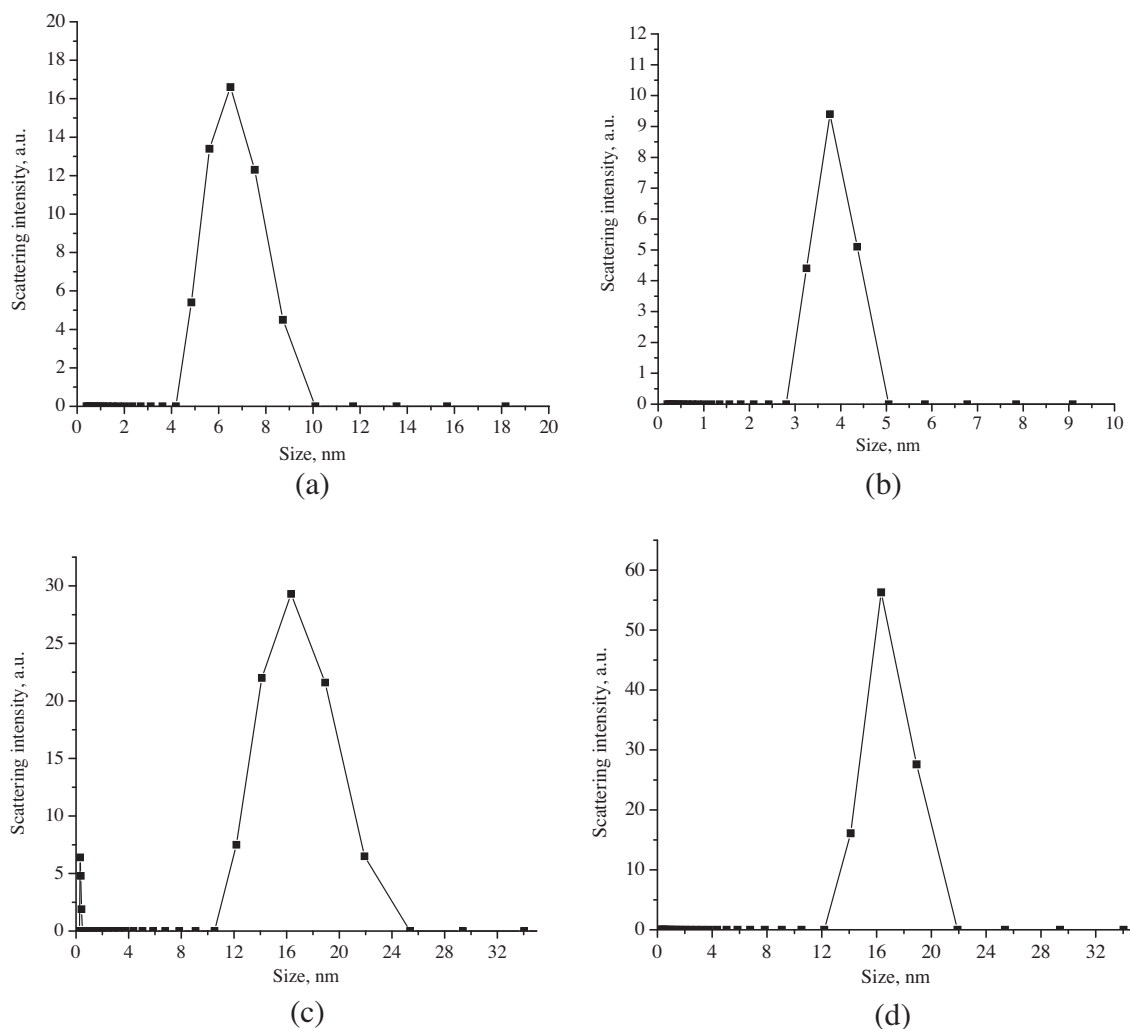


Fig. 5. Plot of scattering intensity vs. size of the silver nanoparticle for (a) C_{60} ($1.0 \times 10^{-5} \text{ mol dm}^{-3}$) + AgNp, (b) C_{70} ($1.0 \times 10^{-5} \text{ mol dm}^{-3}$) + AgNp, (c) **1** ($3.750 \times 10^{-6} \text{ mol dm}^{-3}$) + C_{60} ($7.750 \times 10^{-5} \text{ mol dm}^{-3}$) + AgNp and (d) **1** ($3.750 \times 10^{-6} \text{ mol dm}^{-3}$) + C_{70} ($7.050 \times 10^{-5} \text{ mol dm}^{-3}$) + AgNp systems.

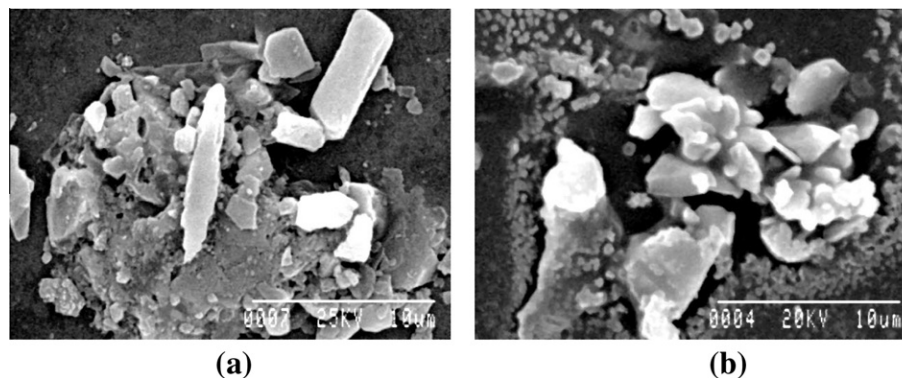


Fig. 6. SEM photographs of (a) C_{70} ($7.050 \times 10^{-5} \text{ mol dm}^{-3}$) + **1** ($3.750 \times 10^{-6} \text{ mol dm}^{-3}$) + AgNp system and (b) C_{60} ($7.475 \times 10^{-5} \text{ mol dm}^{-3}$) + **1** ($3.750 \times 10^{-6} \text{ mol dm}^{-3}$) + AgNp system recorded in toluene.

Conductance measurements

Conductance measurements of the **1** in presence of only AgNp, only C_{60} , only C_{70} , C_{60} + AgNp and C_{70} + AgNp mixtures reveal very important new physicochemical aspect. It is observed that in presence of AgNp, the conductance value of **1** in toluene gets very little change with increasing time. After 3 h of measurement, the conductance value of the mixture of **1** and AgNp in toluene is determined to be $0.4 \mu\text{S}$ compared to the initial value of $0.2 \mu\text{S}$ in absence of AgNp (see Table 1S). This observation is quite consistent with the fact that AgNp fails to generate any photocurrent during its interaction with porphyrin. On the other hand, the conductance measurement of C_{60} + **1** (Table 2S) and C_{70} + **1** (Table 3S) mixtures in absence of AgNp, reveal considerable increase in the value of such parameter with increase in time. The conductance value of C_{60} –**1** system is estimated to be $1.0 \mu\text{S}$ after 41.0 min of measurement. In presence of AgNp, the conductance value of the same system is reduced to $0.6 \mu\text{S}$ after same time interval (see Table 4S). This phenomenon gives clear evidence in favor of the inhibition of complexation between **1** and C_{60} in presence of AgNp. Similar sort of experimental observations are noticed in case of C_{70} –**1** system in absence and presence of AgNp (see Table 5S).

SEM Measurements

SEM measurements of **1** in presence of AgNp reveals uneven sized particles (Fig. 8S). The SEM image of C_{70} + **1** + AgNp composite mixture (Fig. 6(a)) obtained from drop-casted films of the clusters ($[\mathbf{1}]:[C_{70}] = 1:1$) on a stab made of copper reveals the exclusive formation of rod-like clusters with a well-controlled size ($15\text{--}20 \text{ nm}$ in the long axis). In sharp contrast, the SEM image of the clusters of (C_{60} + **1** + AgNp) (Fig. 6(b)) shows ill-defined sizes and shapes. In particular, the SEM image of clusters of (C_{60}) reveals both rods of different sizes ($15\text{--}20 \text{ nm}$ in the long axis) and small random-shaped structures ($1\text{--}5 \text{ nm}$). In addition, variation of the $[\mathbf{1}]:[C_{60}]$ ratio is found to affect the cluster size and shape (Fig. 6(b)). This trend is consistent with the size of the large and bucket-shaped surface holes, which are expected to incorporate up to as many as C_{60} molecules. These results clearly demonstrate that the shape and the size of the surface holes on the **1**-C(60/70)-AgNp structure play an important role in controlling the formation of molecular clusters with either C_{60} or C_{70} molecules.

Theoretical calculations

Table 1 reports the K values of various fullerene-**1** complexes. The notable feature of the binding studies is that, presence of

Table 2

Heat of formation (ΔH_f^0) value for C_{60} –**1** and C_{70} –**1** complexes done by MMMF calculations in vacuo.

System	ΔH_f^0 , kJ mol^{-1}
C_{60} – 1	–62.60
C_{70} – 1 (side-on orientation of C_{70})	–68.95
C_{70} – 1 (end-on orientation of C_{70})	–61.35

AgNp in the fullerene-**1** composite mixture causes moderate increase in the selectivity of binding of C_{70} over C_{60} , i.e., $K_{C_{70}}/K_{C_{60}}$; $K_{C_{70}}/K_{C_{60}}$ is estimated to be ~ 10.1 in presence of AgNp, while the same parameter exhibits value of ~ 9.6 when it is measured in absence of AgNp. It is observed that for all the complexes studied, C_{70} exhibits largest value of K in comparison to C_{60} . Very large value of average selectivity in binding in absence of AgNp suggests that **1** may discriminate C_{60} and C_{70} from their mixture in solution. Large value of K for the C_{70} –**1** system, both in absence and in presence of AgNp, provides additional stabilization to that system and such a stabilization of the C_{70} –**1** supra-molecular complex may be attributed due to the presence of intermolecular interaction between the graphitic 6:6 plane of C_{70} and the monoporphyrin. Primarily, the attractive interaction between C_{70} and the monoporphyrin is driven by the presence of dispersive forces associated with Π – Π interactions. The most concrete evidence of the above statement is illustrated by the side-on rather than end-on binding of C_{70} with the plane of **1**. Molecular mechanics calculations by force field model (MMMF) calculations in vacuo well reproduce the above feature regarding orientation of bound guest (here C_{60} and C_{70}) with the plane of **1**. Thus, in the case of C_{70} –**1** complex, the side-on interaction of C_{70} with **1** generates enthalpies of formation (ΔH_f^0) value of $-68.95 \text{ kJ mol}^{-1}$ (Table 2). However, the end-on pattern of C_{70} molecule produces ΔH_f^0 value of $-61.35 \text{ kJ mol}^{-1}$ (Table 2). It is already well established that the 6:6 ring-juncture bond of the C_{70} , rather than 6:5 ring-juncture bond, lies closest to the porphyrin plane as the 6:6 “double” bonds of C_{70} are more electron-rich than 6:5 “single” bonds [10,35]. Thus, the equatorial face of C_{70} is centered over the electropositive center of the porphyrin plane, which can be viewed as an enhancement in van der Waals interaction due to availability of greater surface area and volume (see Table 2) favoring strong Π – Π interactions. It should be noted at this point that C_{60} –**1** complex exhibits much lower value of ΔH_f^0 , viz., $-62.60 \text{ kJ mol}^{-1}$ compared to C_{70} –**1** complex as listed in Table 2. Single projection geometric structures for all the fullerene-**1** complexes at their different orientations are visualized in Fig. 7.

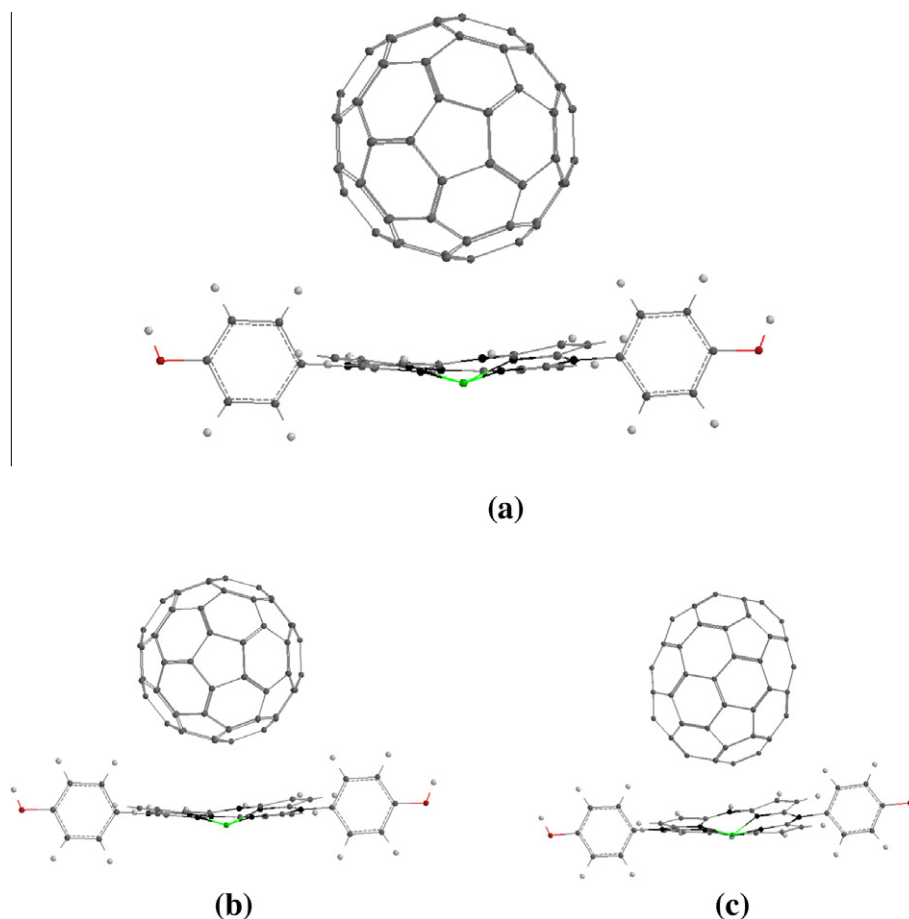


Fig. 7. Single projection geometric structures for (a) C₆₀-**1**, (b) C₇₀-**1** (side-on orientation of C₇₀) and (c) C₇₀-**1** (end-on orientation of C₇₀) done by MMMF calculations in vacuo.

Conclusions

The main results of our attempt to develop a new and improved methodology of characterization of fullerene-porphyrin non-covalent assembly in presence of silver nanoparticles are summarized below:

- (1) The two most important as well as new photophysical insights of the present investigations are the increase in the absorbance value of the Soret absorption band of **1** after complexation with C₆₀ and C₇₀ in presence of AgNp relative to the situation when complexation between fullerenes and **1** takes place in absence of AgNp, and secondly, quenching efficiencies of both C₆₀ and C₇₀ have been reduced in presence of AgNp in toluene
- (2) Estimation of binding constants applying steady state fluorescence spectroscopic techniques reveal that **1** could not serve as an efficient complexing agent towards C₆₀ and C₇₀ in presence of AgNp; however, **1** serves as a better discriminator molecule towards C₇₀ in presence of AgNp.
- (3) DLS studies establish the fact that particle size of AgNp becomes larger when complexation takes place between fullerenes and **1**, and it is the primary reason behind getting lesser magnitude of K value for fullerene-**1** systems.
- (4) Conductance measurements evoke that AgNp particle reduces the magnitude of conductance value for the fullerene-**1** systems in presence of AgNp.

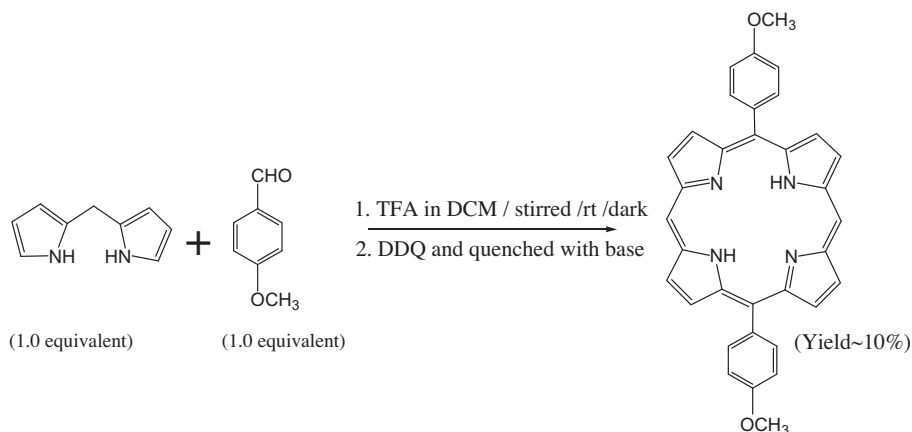
- (5) SEM measurements prove that the shape and the size of the surface holes on the fullerene-porphyrin-AgNp structure play an important role in controlling the formation of molecular clusters with fullerenes.
- (6) Theoretical calculations well reproduce the geometric structures of the fullerene-**1** complexes and interpret the stability difference between C₆₀ and C₇₀ complexes of **1**.
- (7) The results emanating from present investigations would be of potential interest in studying the interaction between fullerenes and diporphyrin in presence of silver nanoparticles in near future.

Acknowledgments

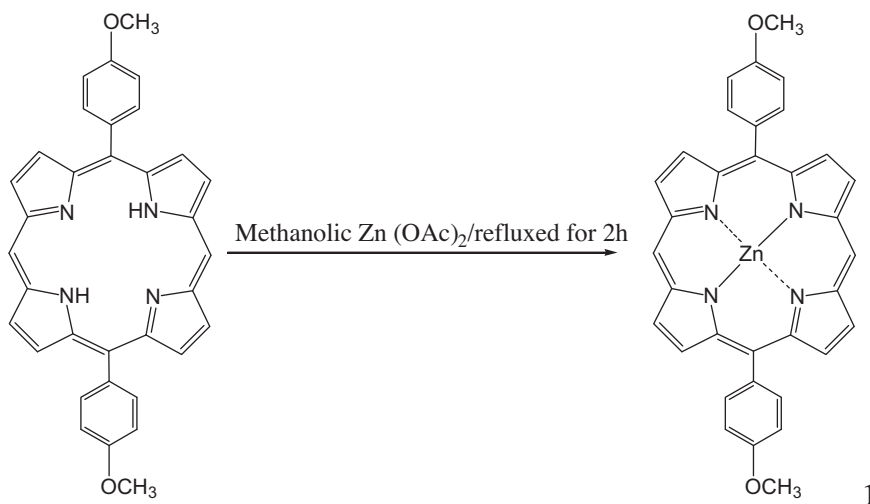
RM thanks Department of Atomic Energy, Board of Research in Nuclear Science (BRNS), Bhabha Atomic Research Centre, Mumbai, India for providing Junior Research Fellowship to him. Financial assistance through the project of Ref. No. 2010/20/37P/2/BRNS is also gratefully acknowledged.

Appendix A

The synthetic schemes are shown in Schemes 1 and 2.



Scheme 1. Synthesis of 5, 15-di (para-methoxy phenyl)-porphyrin.



Scheme 2. insertion of Zn metal in 5, 15-di (para-methoxy phenyl)-porphyrin.

Appendix B. Supplementary data

Supplementary data associated with this article can be found, in the online version, at <http://dx.doi.org/10.1016/j.saa.2012.05.040>.

References

- [1] A. Hagfeldt, M. Grätzel, *Acc. Chem. Res.* 33 (2000) 269–277.
- [2] M. Grätzel, *Nature* 414 (2001) 338–345.
- [3] J.-F. Eckert, J.-F. Nicoud, J.-F. Nierengarten, S.-G. Liu, L. Echegoyen, F. Barigelletti, N. Armaroli, L. Ouali, V. Krasnikov, G. Hadziioannou, *J. Am. Chem. Soc.* 122 (2000) 7467–7479.
- [4] R. Ziessel, A. Harriman, *Chem. Commun.* 47 (2011) 611–631.
- [5] D. Gust, T.A. Moore, A.L. Moore, *Acc. Chem. Res.* 34 (2001) 40–48.
- [6] K. Li, D.I. Schuster, D.M. Guldi, M.A. Herranz, L. Echegoyen, *J. Am. Chem. Soc.* 126 (2004) 3388–3389.
- [7] F. D'Souza, P.M. Smith, M.E. Zandler, A.L. McCarty, M. Itou, Y. Araki, O. Ito, *J. Am. Chem. Soc.* 126 (2004) 7898–7907.
- [8] N. Armaroli, G. Marconi, L. Echegoyen, J.-P. Bourgeois, F. Diederich, *Chem.-Eur. J.* 6 (2000) 1629–1645.
- [9] H. Imahori, *J. Phys. Chem. B* 108 (2004) 6130–6143.
- [10] D. Sun, F.S. Tham, C.A. Reed, L. Chaker, M. Burgess, P.D.W. Boyd, *J. Am. Chem. Soc.* 122 (2000) 10704–10705.
- [11] Y. Shoji, K. Tashiro, T. Aida, *J. Am. Chem. Soc.* 126 (2004) 6570–6571.
- [12] F. Diederich, M. Gómez-López, *Chem. Soc. Rev.* 28 (1999) 263–277.
- [13] P.D.W. Boyd, M.C. Hodgson, C.E.F. Rickard, A.G. Oliver, L. Chaker, P.-J. Brothers, R.D. Bolskar, F.S. Tham, C.A. Reed, *J. Am. Chem. Soc.* 121 (1999) 10487–10495.
- [14] P.D.W. Boyd, C.A. Reed, *Acc. Chem. Res.* 38 (2005) 235–242.
- [15] D.M. Guldi, *Chem. Soc. Rev.* 31 (2002) 22–36.
- [16] L. Sherwood, in: P. Adams, N. Rose (Eds.), *Fundamentals of Physiology, A Human Perspective*, Thomson Brooks/Cole, USA, 2006.
- [17] H. Scheer (Ed.), *Chlorophylls*, CRC Press, Boca Raton/Ann Arbor/Boston/London, 1991.
- [18] J.D. Regan, J.A. Parrish (Eds.), *The Science of Photomedicine*, Plenum, New York/London, 1982.
- [19] M. Pelton, J. Aizpurua, G. Bryant, *Laser & Photon Rev.* 2 (2008) 136–159.
- [20] P.K. Jain, X. Huang, I.H. El-Sayed, M.A. El-Sayed, *Acc. Chem. Res.* 41 (2008) 1578–1586.
- [21] E. Hutter, J.H. Fendler, *Adv. Mater.* 16 (2004) 1685–1706.
- [22] T. Hasobe, H. Imahori, P.V. Kamat, T.K. Ahn, S.K. Kim, D. Kim, A. Fujimoto, T. Hirakawa, S. Fukuzumi, *J. Am. Chem. Soc.* 127 (2005) 1216–1228.
- [23] A. Kotiaho, R.M. Lahtinen, H.-K. Latvala, A. Efimov, N.V. Tkachenko, H. Lemmetyinen, *Chem. Phys. Lett.* 471 (2009) 269–275.
- [24] A. Kotiaho, R.M. Lahtinen, N.V. Tkachenko, A. Efimov, A. Kira, H. Imahori, H. Lemmetyinen, *Langmuir* 23 (2007) 13117–13125.
- [25] F. Sedona, M.D. Marino, M. Sambì, T. Carofoglio, E. Lubian, M. Casarin, E. Tondello, *ACS Nano* 4 (2010) 5147–5154.
- [26] R.F. Aroca, R.A.A. -Puebla, N. Pieczonka, S.S. -Cortez, J.V.G. -Ramos, *Adv. Colloid. Interface Sci.* 116 (2005) 45–61.
- [27] H. Imahori, Y. Sakata, *Eur. J. Org. Chem.* (1999) 2445–2557.
- [28] I.B. Martini, B. Ma, T.D. Ros, R. Helgeson, F. Wudl, B.J. Schwartz, *Chem. Phys. Lett.* 327 (2000) 253–262 (and the references cited there in).
- [29] D.I. Schuster, P. Cheng, S.R. Wilson, V. Prokhorenko, M. Katterle, A.R. Holzwarth, S.E. Braslavsky, G. Klichm, R.M. Williams, C. Luo, *J. Am. Chem. Soc.* 121 (1999) 11599–11600.
- [30] D. Gust, T.A. Moore, A.L. Moore, D. Kuciauskas, P.A. Liddell, B.D. Halbert, *J. Photochem. Photobiol. B* 43 (1998) 209–216.
- [31] G. Yin, D. Xu, Z. Xu, *Chem. Phys. Lett.* 365 (2002) 232–236.
- [32] R. Pecora, *J. Nanoparticle. Res.* 23 (2000) 123–131.
- [33] L.S. Ehrlich, T. Liu, S. Scarlata, B. Chu, C.A. Carter, *Biophys. J.* 81 (2001) 586–594.
- [34] W. Brown, *Dynamic Light Scattering: The Method and Some Applications*, Clarendon Press, Oxford, 1993.
- [35] D. Sun, F.S. Tham, C.A. Reed, P.D.W. Boyd, *Proc. Natl. Acad. Sci. USA* 99 (2002) 5088–5092.